

## A Precipitator for the Detection of Thiophilic Metals in Aqua

Tobin J. Dickerson,<sup>†</sup> Neal N. Reed,<sup>†</sup> James J. LaClair,<sup>\*,‡</sup> and Kim D. Janda<sup>\*,†</sup>

Contribution from the Department of Chemistry and The Skaggs Institute for Chemical Biology, The Scripps Research Institute, 10550 North Torrey Pines Road, La Jolla, California 92037, and Xenobe Research Institute, P.O. Box 4073, San Diego, California 92164-4073

Received July 13, 2004; Revised Manuscript Received September 29, 2004; E-mail: kjanda@scripps.edu; i@xenobe.org

**Abstract:** The detection of toxic metals including mercury and lead has become a vital analytical tool for environmental remediation and regulation of food stocks. A prevalent obstacle with the current assessment of metal ion contamination originates from the lack of adequate assay throughput. In this context, a critical concern with current analyses stems from the fact that the majority of these assays are solution-based, and thus the response is highly dependent upon the assay environment. Herein, we describe a fluorescent dye-doped crystalline assay that offers convincing metal selection and provides detection comparable to conventional solution-based ligands used for the spectrofluorometric analysis of thiophilic heavy metal ions. While comparable in analytical performance to known methodologies, the formation of crystalline analytes provides for signal amplification and, consequently, a powerful platform whose analysis is directly amenable to high-throughput video capture systems. This procedure has been tested in a variety of scenarios and shows good performance using readily available equipment, including a commercially available Universal Serial Bus (USB) CCD camera. Furthermore, when developed in a microcapillary format, this assay is capable of screening thousands of samples per day for the presence of subnanomolar concentrations of Hg<sup>2+</sup> using a conventional fluorescence microscope.

### Introduction

The introduction of heavy metals into the environment has occurred in tandem with the emergence of the tools of modern society, including automobiles, industrial activities, and the burning of coal.<sup>1</sup> Consequently, the detection of these metals has attained significant prominence within the scientific community and the public consciousness as a result of their varied deleterious biological activities. These concerns have been furthered by the discovery that aquatic organisms convert elemental mercury to methylmercury, which subsequently concentrates through the food chain in the tissues of fish and marine mammals.<sup>2</sup> Unquestionably, the development of facile and efficient methodologies for the detection of heavy metals in a wide range of settings is paramount in the effort to minimize incidences of mortality attributable to heavy metal toxicity.

A plethora of indicators are known to detect metal ions through the intramolecular modulation of a pendant chromophore.<sup>3</sup> While effective for toxic metal analysis in laboratory environments,<sup>4</sup> few of these probes have proven suitable for screening within modern industrial settings.<sup>5</sup> While the design of colorimetric ligation has been critically evaluated by Lippard, Haugland, and others,<sup>3,6</sup> the predominant theme within metal ion sensing relies on solution-based chemistry. Few efforts have

correlated metal ion sensing with material synthesis (i.e., crystallization, precipitation, or polymerization).

Recent advances in the study of colorimetric ligands suggest that a viable metal indicator offers (1) the appropriate direction of metal-mediated modulation, (2) a high degree of sensitivity, and (3) a defined metal selectivity. We have demonstrated that correlation of ligation-induced colorimetric response with precipitation provides an effective vector for metal ion analysis.<sup>3b</sup> Here, amplification of a colorimetric response through precipitation provided a practical screen for mercuric ion. We now report that the appendage of a colorimetric moiety is unnecessary for the analysis of thiophilic metals and adapt this to provide a digital screen for the analysis of Hg<sup>2+</sup>, Pb<sup>2+</sup>, and Cd<sup>2+</sup>.

### Results and Discussion

The construct began with the synthesis of dithiophthalides **3**.<sup>7</sup> As shown in Figure 1, **3a** and **3b** were prepared from phthalic

<sup>†</sup> Department of Chemistry and The Skaggs Institute for Chemical Biology, The Scripps Research Institute.

<sup>‡</sup> Xenobe Research Institute.

- (1) (a) Shotyck, W.; Weiss, D.; Appleby, P. G.; Cheburkin, A. K.; Frei, R.; Gloor, M.; Kramers, J. D.; Reese, S.; Vanderknaap, W. O. *Science* **1998**, *281*, 1635–1640. (b) Benoit, J. M.; Fitzgerald, W. F.; Damman, A. W. *Environ. Res.* **1998**, *78*, 118–133.
- (2) Nendza, M.; Herbst, T.; Kussatz, C.; Gies, A. *Chemosphere* **1997**, *35*, 1875–1885.

- (3) (a) Choi, M. J.; Kim, M. Y.; Chang, S.-K. *Chem. Commun.* **2001**, 1664–1665. (b) Brümmer, O.; La Clair, J. J.; Janda, K. D. *Org. Lett.* **1999**, *1*, 415–418. (c) Sancenón, F.; Martínez-Mañez, R.; Soto, J. *Chem. Commun.* **2001**, 2262–2263. (d) Sancenón, F.; Martínez-Mañez, R.; Soto, J. *Tetrahedron Lett.* **2001**, *42*, 4321–4323. (e) Moon, S. Y.; Cha, N. R.; Kim, Y. H.; Chang, S. K. *J. Org. Chem.* **2004**, *69*, 181–183. (f) Palomares, E.; Vilar, R.; Durrant, J. R. *Chem. Commun.* **2004**, 362–363. (g) Kuhn, M. A.; Hoyland, B.; Carter, S.; Zhang, C.; Haugland, R. P. *Proc. SPIE, Intl. Soc. Opt. Eng.* **1995**, 2388, 238–242.
- (4) (a) Baeumner, A. *J. Anal. Bioanal. Chem.* **2003**, *377*, 434–445. (b) Epstein, J. R.; Walt, D. R. *Chem. Soc. Rev.* **2003**, *32*, 203–214. (c) Jain, K. K. *Med. Device Technol.* **2003**, *14*, 10–15. (d) Ulber, R.; Frerichs, J. G.; Beutel, S. *Anal. Bioanal. Chem.* **2003**, *376*, 342–348.
- (5) Roblin, P.; Barrow, D. A. *J. Environ. Monit.* **2000**, *2*, 385–92.
- (6) (a) Descalzo, A. B.; Martínez-Mañez, R.; Radeglia, R.; Rurack, K.; Soto, J. *J. Am. Chem. Soc.* **2003**, *125*, 3418–3419. (b) Nolan, E. M.; Lippard, S. J. *J. Am. Chem. Soc.* **2003**, *125*, 14270–14271. (c) Xu, X.; Thundat, T. G.; Brown, G. M.; Ji, H. F. *Anal. Chem.* **2002**, *74*, 3611–3615. (d) Zhang, X. B.; Guo, C. C.; Li, Z. Z.; Shen, G. L.; Yu, R. Q. *Anal. Chem.* **2002**, *74*, 821–825.

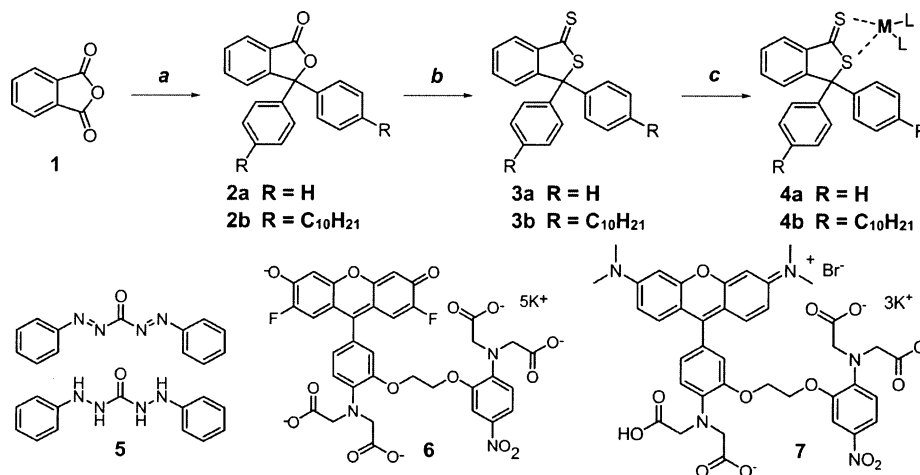


**Figure 1.** Synthesis of thiophilic ligands **3** and comparison of their structures to established indicators **5–7**. (a) i,  $\text{ArMgBr}$ ,  $\text{C}_6\text{H}_6$ ,  $80^\circ\text{C}$ , 24 h; ii, 2 M HCl; iii,  $\text{N}_2\text{H}_4\cdot\text{H}_2\text{O}$ , EtOH,  $78^\circ\text{C}$ , 24 h. (b)  $\text{P}_4\text{S}_{10}$ , xylene,  $140^\circ\text{C}$ , 18 h. (c)  $\text{M}^{n+}(\text{OAc})_n$  or  $\text{M}^{n+}\text{Cl}_n$ ,  $\text{H}_2\text{O}$ ,  $\text{CH}_3\text{CN}$ , < 1 min.

anhydride (**1**) in two operations.<sup>8</sup> Initial addition to the anhydride by phenylmagnesium bromide was followed by addition of a second equivalent of phenylmagnesium bromide and subsequent intramolecular ester formation to give lactone **2a**. Compound **2a** could then be smoothly converted to xanthane **3a** by treatment with  $\text{P}_4\text{S}_{10}$  in refluxing xylenes. Importantly, the entire route to **3a** could be executed at the kilogram scale without chromatographic purification.

When presented to a panel of metal ions, **3a** complexed and precipitated  $\text{Hg}^{2+}$ ,  $\text{Pb}^{2+}$ ,  $\text{Cd}^{2+}$ ,  $\text{Au}^{3+}$ ,  $\text{Cu}^{2+}$ ,  $\text{Pd}^{2+}$ ,  $\text{Ni}^{2+}$ ,  $\text{Co}^{2+}$ ,  $\text{Mo}^{2+}$ , and  $\text{Pt}^{2+}$ . Job plots indicated that precipitates **4a** ( $\text{M} = \text{Hg}^{2+}$ ,  $\text{Pb}^{2+}$ ,  $\text{Cd}^{2+}$ ) existed as a 1:1 complex. A 2:1 ligand to metal complex could also be formed when precipitating from solutions containing  $>5$  mM **3a**. In contrast, the precipitation of **3b** by  $\text{Hg}^{2+}$  and  $\text{Pb}^{2+}$  required over 5 min for induction, and other metals including  $\text{Cd}^{2+}$  failed to provide sufficient yields of precipitate. Consequently, we deemed that the solubility of **3b** and its metal complexes do not provide a response adequate for analytical use.

Solubility products were determined using conventional mass analysis to characterize the metal ion selection of **3a** (Figure 2A). Alternatively, the precipitation of **4a** could be determined by measuring the spectrophotometric loss of **3a** in the supernatant at  $\lambda_{\text{max}} = 304$ , 330, or 356 nm (Figure 2B). Quantitative analysis with **3a** was comparable in accuracy and precision to assays developed with conventional ligands, including diphenylcarbazone **5**, Fluo-5N **6**, and Rhod-5N **7**.<sup>9</sup> The precipitation of **3a** in 10% aqueous  $\text{CH}_3\text{CN}$  was visually apparent upon addition of  $2\ \mu\text{M}$   $\text{Hg}(\text{OAc})_2$  to  $1\ \mu\text{M}$  **3a**,  $50\ \mu\text{M}$   $\text{CdCl}_2$  to  $25\ \mu\text{M}$  **3a**, and  $10\ \mu\text{M}$   $\text{Pb}(\text{OAc})_2$  to  $5\ \mu\text{M}$  **3a**. The precipitation of **4a** with  $\text{Hg}^{2+}$ ,  $\text{Pb}^{2+}$ , or  $\text{Cd}^{2+}$  was tolerant of alkali metals ( $\text{Na}^+$ ,  $\text{K}^+$ ), alkaline earth metals ( $\text{Ca}^{2+}$ ,  $\text{Mg}^{2+}$ ), and transition metals ( $\text{Mn}^{2+}$ ,  $\text{Mo}^{2+}$ ,  $\text{Cr}^{2+}$ , and  $\text{Fe}^{2+}$ ), as given by the modest change

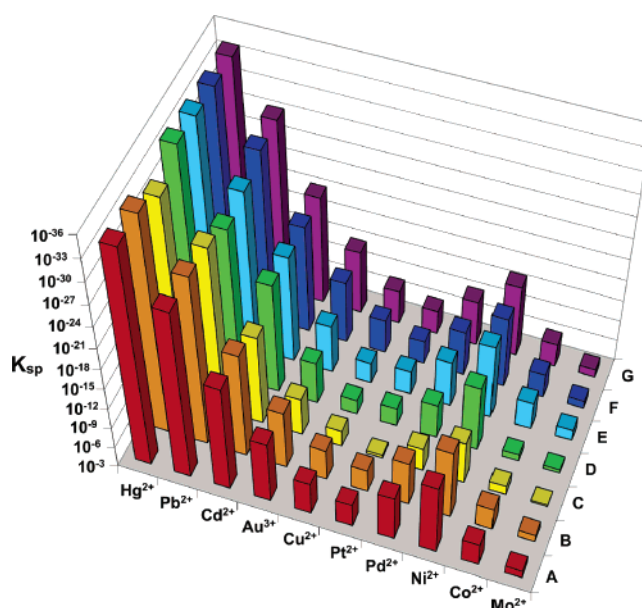


**Figure 2.** Solubility products ( $K_{\text{sp}}$ ) of metal complexes of **3a** as determined by (A) the mass of precipitate **4a**, (B) spectroscopic loss of **3a**, (C) the mass of **4a** obtained in the presence of  $10^5$  molar equiv of  $\text{Li}^+$ ,  $\text{Na}^+$ ,  $\text{K}^+$ ,  $\text{Cs}^+$ ,  $\text{Mg}^{2+}$ ,  $\text{Ca}^{2+}$ ,  $\text{Ba}^{2+}$ ,  $\text{V}^{2+}$ ,  $\text{Cr}^{2+}$ ,  $\text{Mn}^{2+}$ ,  $\text{Fe}^{2+}$ ,  $\text{Co}^{2+}$ ,  $\text{Rh}^{3+}$ ,  $\text{Zn}^{2+}$ ,  $\text{Al}^{3+}$ ,  $\text{Sn}^{2+}$ ,  $\text{As}^{3+}$ ,  $\text{Sb}^{3+}$ ,  $\text{Bi}^{3+}$ ,  $\text{La}^{3+}$ ,  $\text{Ce}^{3+}$ ,  $\text{Sm}^{3+}$ ,  $\text{Eu}^{3+}$ , and  $\text{Yb}^{3+}$ . The solubility product could also be determined using a digital displacement map analysis as given by imaging (D) with a CCD microscope (Intel Digital Blue), (E) on an inverted microscope (Nikon Eclipse TE300), (F) with fluorescence crystals of **4a** (Figure 3E), and (G) with fluorescent crystals of **4a** grown in capillaries (Figure 3G).

in  $K_{\text{sp}}$  when complexes of **4a** were formed in the presence of  $10^5$  molar excesses of nonbinding metal ions (Figure 2C). This selection permitted the analysis of  $\text{Hg}^{2+}$ ,  $\text{Pb}^{2+}$ , and  $\text{Cd}^{2+}$  in mixtures containing 500 equiv of  $\text{Cu}^{2+}$  in contrast to established indicators for  $\text{Hg}^{2+}$  such as Rhod-5N **6**, which typically offer only a 3–5-fold selection for  $\text{Hg}^{2+}$  over  $\text{Cu}^{2+}$ .

Metal selectivity is not the *only* criteria required for a practical screen. Many indicators, including **5–7**, are sensitive to pH, ion strength, impurities, buffers, and solvents. Deviations in these environmental factors can alter the kinetics of ligand association or the photophysical properties of the appended reporter. These complications are furthered by fact that the concentration profile of many solution-based colorimetric ligands remains nonlinear. For instance, the affinity of Fluo-

(7) (a) Szurdoki, F.; Kido, H.; Hammock, B. D. *Bioconjugate Chem.* **1995**, *6*, 145–149. (b) Lo, J.-M.; Lee, J.-D. *Anal. Chem.* **1994**, *66*, 1242–1248. (c) Sachsenberg, S.; Klenke, T.; Krumbein, W. E.; Zeeck, E. *J. Fresenius Anal. Chem.* **1992**, *342*, 163–166. (d) Bond, A. M.; Scholz, F. *J. Phys. Chem.* **1991**, *95*, 7460–7465.

(8) (a) Nugara, P. N.; Huang, N. Z.; Lakshminantham, M. V.; Cava, M. P. *Heterocycles* **1991**, *32*, 1559–1561. (b) Oparin, D. A.; Kuznetsova, A. S. *Vestsi Akademii Navuk BSSR, Seriya Khim. Navuk* **1990**, *6*, 109–110.

(9) Indicators **5–7** displayed high affinities ( $K_{\text{d}} = 10^{-9}$ – $10^{-12}$  M<sup>-1</sup>) to  $\text{Hg}^{2+}$ ,  $\text{Pd}^{2+}$ , and  $\text{Co}^{2+}$  and permitted detection of micromolar levels of these metal ions in the presence of  $10^3$  equiv of nonbinding metals. See: Haugland, R. *Handbook of Fluorescent Probes and Research Products*, 9th ed.; Molecular Probes: Eugene, OR, 2001; Section 20.

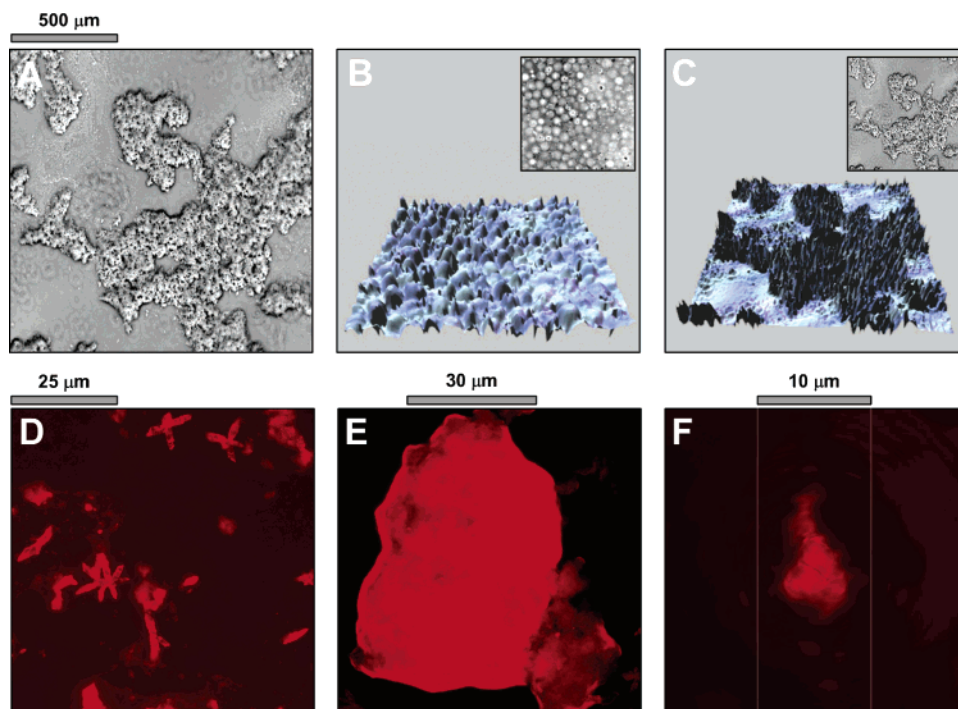


**Figure 3.** Microscopic analysis. (A) The precipitate generated by mixing  $2 \mu\text{M}$   $\text{Hg}(\text{OAc})_2$  with  $1 \mu\text{M}$  **3a** in 10% aqueous  $\text{CH}_3\text{CN}$ , (B) an image (inset) and the Delaunay triangulation map of  $100 \mu\text{m}$  microspheres, (C) an image (inset) and Delaunay map of precipitates **4a** ( $\text{M} = \text{Hg}$ ), (D) fluorescent microcrystals **4a** generated by the mixing of  $1 \text{mM}$   $\text{Hg}(\text{OAc})_2$ ,  $1 \text{mM}$  **3a**, and  $0.5 \mu\text{M}$  Rhod-5N, (E) globular crystals formed from  $20 \text{mM}$   $\text{Hg}^{2+}$ ,  $20 \text{mM}$  **3a**, and  $0.5 \mu\text{M}$  Rhod-5N, (F) a single fluorescent crystal of **4a** ( $\text{M} = \text{Hg}$ ) generated in capillaries by placing a  $1 \pm 0.05 \text{mm}$  long section of  $10 \mu\text{m}$  i.d. fused silica capillary containing  $200 \mu\text{M}$  **3a** and  $2 \mu\text{M}$  rhodamine B in  $\text{CH}_3\text{CN}$  into a  $100 \mu\text{L}$  aliquot of  $0.2 \text{nM}$   $\text{Hg}(\text{OAc})_2$ . Images were collected on a Nikon Eclipse TE300 using Y-2E/C (560BP40 excitation and 595 LP 630/60 BP emission) filter. Comparable images were also generated when precipitating with equimolar amounts of  $\text{Pb}(\text{OAc})_2$ ,  $\text{Cd}(\text{OAc})_2$ ,  $\text{HgCl}_2$ ,  $\text{PbCl}_2$ , and  $\text{CdCl}_2$ .

5N **6** to  $\text{Cd}^{2+}$  is 10-fold larger than  $\text{La}^{3+}$  at  $1 \mu\text{M}$ , while the affinity for the complexes changes to favor  $\text{La}^{3+}$  by 2-fold over  $\text{Cd}^{2+}$  at  $100 \mu\text{M}$ .<sup>3b,9</sup> The fact that  $K_{\text{sp}}$  values (Figure 2A–C) were reproducible within 1% deviation over a wide range of concentrations ( $1 \text{mM}$  to  $0.1 \mu\text{M}$ ), pH (3–10), and temperature ( $0$ – $50 \text{ }^\circ\text{C}$ ) indicated that the precipitation of **3a** offered increased resistance to environmental factors relative to comparable solution-based methodologies. This does not imply, however, that a precipitation-based assay can supplant existing solution technologies for heavy metal detection. Current fluorescent probes that operate in solution are directly amenable to in situ analysis and thus can assay samples that cannot be removed from their natural environment. In contrast, our precipitation-based methodology is very resistant to signal degradation by environmental factors (vide supra), yet requires extraction of the sample from its environment for testing.

The formation of metal precipitates was rapidly screened using high-throughput video-capture techniques. When conducted on a glass slide or in a fused-silica capillary, crystals **4a** ( $\text{M} = \text{Hg}^{2+}$ ,  $\text{Pb}^{2+}$ , or  $\text{Cd}^{2+}$ ) associated on the surface of a glass slide or wall of a capillary within a few seconds after formation (Figure 3). Elemental analysis of the resulting supernatant indicated that the mercuric ion was quantitatively removed from the solution during this process. Indeed, vapor atomic absorption measurements demonstrated that the amount of  $\text{Hg}^{2+}$  ( $0.58 \pm 0.03 \mu\text{M}$ ) after reacting  $6.7 \pm 0.01 \text{mM}$   $\text{Hg}(\text{OAc})_2$  with an  $6.7 \pm 0.01 \text{mM}$  **3a** was well below the error threshold of the pipettors used to prepare the reaction ( $\pm 0.1 \text{mL}$  or  $\pm 4 \mu\text{M}$ ). To improve visualization, the crystals were doped with a fluorescent dye, as given by the addition of  $10^{-3}$  equiv of

Rhod5N or rhodamine B during precipitation to yield needles (Figure 3D) or globular crystals (Figure 3E).

A digital displacement map method was developed to determine the mass of precipitate within each image. A Delaunay triangulation<sup>10</sup> was used to transpose each image (Figure 3) into a 3D vector map.<sup>11</sup> This process provided a net volume of precipitate generated per image using vector analysis. This volume deviated  $3.9 \pm 1.5$  and  $6.1 \pm 2.2\%$  when imaging standard  $100 \mu\text{m}$  microspheres (Figure 3B), on an inverted microscope (Nikon Eclipse TE300) or inexpensive CCD microscope (Intel Digital Blue), respectively. Once calibrated with microspheres, the volumes of precipitates were quickly determined from images of precipitates **4a** (Figure 3C inset) and their corresponding 3D maps (Figure 3C). Using the conditions described in Figure 3A, the CCD microscope (Figure 2D) and inverted microscope (Figure 2E) provided  $K_{\text{sp}}$  values that were comparable to that obtained by conventional assays (Figure 2A,B).<sup>12</sup>

The method was capable of detecting part per billion levels of thiophilic metals when examined in small volume elements. As shown in Figure 3F, single crystals of **4a** were reproducibly generated upon the addition of microcapillaries filled with **3a** into aqueous solutions of metal ion. Displacement map analysis

(10) (a) Wohlberg, B.; de Jager, G. *IEEE T Image Process.* **1999**, *8*, 1716–1729. (b) Lohner, R. *Finite Elem. Anal. Des.* **1997**, *25*, 111–134.

(11) Zhu, W.; Wang, Y.; Yao, Y.; Chang, J.; Graber, H. L.; Barbour, R. L. *J. Opt. Soc. Am. A* **1999**, *14*, 799–802.

(12)  $K_{\text{sp}}$  values were calculated on the basis of comparison of the measured amount of precipitate generated with the known aliquot of metal ion. The amount of precipitate generated was calculated from the volume of precipitate using a density of 7.3, 3.8, and  $4.3 \text{g/mL}$ , for the precipitate generated by the addition of **3a** to  $\text{Hg}(\text{OAc})_2$ ,  $\text{Pb}(\text{OAc})_2$ , and  $\text{CdCl}_2$ , respectively. An average of 20 repetitions was provided.

indicated that the crystal in Figure 3F contained  $16.5 \pm 2.9$  fmol of **4a**. Assuming a 1:1 complex, this finding represented the detection of  $0.17 \pm 0.3$  nM  $\text{Hg}^{2+}$  (0.3 ppb) and indicated an 82% yield of **4a** upon exposure to a 100  $\mu\text{L}$  aliquot of 0.2 nM  $\text{Hg}^{2+}$ . Using the procedure in Figure 3F, comparable precipitates were obtained when exposed to solutions that contained greater than 0.2 nM (0.4 ppb)  $\text{Hg}^{2+}$ , 1.5 nM (0.31 ppb)  $\text{Pb}^{2+}$ , or 2.5 nM (0.28 ppb)  $\text{Cd}^{2+}$ .

## Conclusion

In summary, we have developed an assay for thiophilic heavy metals that uses precipitation to decrease interference and increase detection. Analysis in droplets or capillaries provides an effective tool for determining the solubility product of metal complexes using femtomoles of ligand **3a**. This assay was conducted with common imaging systems. This finding suggests that the combination of ligand synthesis, crystal engineering, and fluorescent imaging can provide an information-rich platform for toxic metal analyses.

## Experimental Section

**General Methods.** Unless otherwise stated, all reactions were performed under an inert atmosphere with dry reagents and solvents and flame-dried glassware. Analytical thin-layer chromatography (TLC) was performed using 0.25 mm precoated silica gel Kieselgel 60 F<sub>254</sub> plates. Visualization of the chromatogram was by UV absorbance, iodine, dinitrophenylhydrazine, ceric ammonium molybdate, ninhydrin, or potassium permanganate as appropriate. Preparative and semi-preparative TLC was performed using Merck 1 mm or 0.5 mm coated silica gel Kieselgel 60 F<sub>254</sub> plates, respectively. Methylene chloride and chloroform were distilled from calcium hydride. Tetrahydrofuran (THF) was distilled from sodium/benzophenone. Methanol was distilled from magnesium. <sup>1</sup>H and <sup>13</sup>C NMR spectra were recorded on a Varian INOVA-399 spectrometer at 400 and 100 MHz, respectively, and are reported in parts per million, unless otherwise noted. All spectra were processed with 0.5 Hz line broadening. Matrix-assisted laser desorption/ionization (MALDI) FTMS experiments are performed on an IonSpec FTMS mass spectrometer. Electrospray ionization (ESI) mass spectrometry experiments were performed on an API 100 Perkin-Elmer SCIEX single quadrupole mass spectrometer.

**3,3-Diphenylisobenzofuran-1(3H)-one (2a).** To a solution of phthalic anhydride (5 g, 33.8 mmol) in benzene (100 mL), phenylmagnesium bromide (84.5 mmol) was added slowly and the solution heated to reflux for 24 h. The reaction was then cooled and 2 M HCl (100 mL) added slowly. The organic phase was separated, washed with water (3  $\times$  20 mL), dried on  $\text{MgSO}_4$ , and concentrated. The resulting residue was then dissolved in EtOH (75 mL), and hydrazine hydrate (3 mL) was added and heated to reflux for 24 h. The solution was then cooled to 4  $^\circ\text{C}$ , and the resulting yellow crystals were collected and dried in vacuo to give 3.7 g (38%) of the desired lactone **2a**. <sup>1</sup>H NMR ( $\text{CDCl}_3$ , 300 MHz):  $\delta$  7.94 (d,  $J = 7.5$  Hz, 1H), 7.69 (t,  $J = 7.2$  Hz, 1H), 7.58 (d,  $J = 7.5$  Hz, 1H), 7.53 (d,  $J = 7.2$  Hz, 1H), 7.33 (m, 10H). <sup>13</sup>C NMR ( $\text{CDCl}_3$ , 75 MHz):  $\delta$  169.8, 152.0, 141.0, 134.3, 129.5, 128.7, 128.6, 127.3, 126.2, 125.7, 124.4, 92.0. MALDI–FTMS ( $\text{M} + \text{H}^+$ ). Calcd for  $\text{C}_{20}\text{H}_{14}\text{O}_2$ : 287.1067. Found: 287.1058.

**3,3-Diphenylbenzo[*c*]thiophene-1(3H)-thione (3a).** Lactone **2a** (489 mg, 1.71 mmol) was dissolved in xylene (25 mL). To this solution,  $\text{P}_4\text{S}_{10}$  (380 mg, 0.86 mmol) was added and the reaction heated to reflux for 18 h. The solution was then cooled, filtered, and concentrated to give the desired product **3a** in excellent yield (540 mg, 99%). <sup>1</sup>H NMR ( $\text{CDCl}_3$ , 300 MHz):  $\delta$  8.08 (d,  $J = 8$  Hz, 1H), 7.59 (dt,  $J = 0.5$  Hz, 8 Hz, 1H), 7.48 (dt,  $J = 0.5$  Hz, 8 Hz, 1H), 7.30 (m, 11H). <sup>13</sup>C NMR ( $\text{CDCl}_3$ , 75 MHz):  $\delta$  225.5, 153.0, 142.4, 142.0, 132.9, 128.9, 128.7, 128.5, 128.1, 127.6, 125.3. MALDI–FTMS ( $\text{M} + \text{H}^+$ ). Calcd for

$\text{C}_{20}\text{H}_{14}\text{S}_2$ : 319.0610. Found: 319.0609. UV/vis ( $\text{CH}_3\text{CN}$ ):  $\lambda_{\text{max}}$  ( $\epsilon$ ) = 509 (1850), 340 (5600), 220 nm (13000).

**3,3-Bis(4-decylphenyl)isobenzofuran-1(3H)-one (2b).** A solution of 4-decylphenylmagnesium bromide ( $\sim 1$  M in THF) was prepared from magnesium (90 mg, 3.7 mmol) and 4-(decylphenyl)bromide (1 g, 3.4 mmol). This Grignard reagent was added to a solution of phthalic anhydride (201 mg, 1.36 mmol) in toluene (10 mL) and the solution heated to reflux for 24 h. The dark red solution was then cooled to room temperature and quenched with 20% aqueous HCl (10 mL). The organic phase was separated, washed with water (2  $\times$  10 mL), saturated NaCl (10 mL), and concentrated. The resulting residue was then dissolved in EtOH (10 mL), and hydrazine hydrate (1 mL) was added and heated to reflux for 24 h. The reaction was then cooled to room temperature, concentrated in vacuo, and purified by radial chromatography (5:95 EtOAc:hexane) to give 103 mg (14%) of the desired lactone **2b**. <sup>1</sup>H NMR ( $\text{CDCl}_3$ , 500 MHz):  $\delta$  7.93 (dd,  $J = 0.75$  Hz, 7.7 Hz, 1H), 7.67 (dt,  $J = 1.1$  Hz, 7.7 Hz, 1H), 7.55 (m, 2H), 7.23 (d,  $J = 8.2$  Hz, 4H), 7.12 (d,  $J = 8.2$  Hz, 4H), 2.58 (t,  $J = 7.5$  Hz, 4H), 1.59 (m, 5H), 1.29 (m, 32H), 0.88 (t,  $J = 7$  Hz, 6H). <sup>13</sup>C NMR ( $\text{CDCl}_3$ , 125 MHz):  $\delta$  170.4, 152.9, 143.8, 138.6, 134.5, 129.6, 128.8, 127.5, 126.4, 126.1, 124.6, 92.3, 36.0, 32.4, 31.8, 30.1, 30.0, 29.9, 29.8, 23.2, 14.6. MALDI–FTMS ( $\text{M} + \text{H}^+$ ). Calcd for  $\text{C}_{40}\text{H}_{54}\text{O}_2$ : 567.4196. Found: 567.4184.

**3,3-Bis(4-decylphenyl)benzo[*c*]thiophene-1(3H)-thione (3b).** Lactone **2b** (47 mg, 83.0  $\mu\text{mol}$ ) was dissolved in xylene (2 mL). To this solution,  $\text{P}_4\text{S}_{10}$  (30 mg, 67.6  $\mu\text{mol}$ ) was added and the reaction heated to reflux for 18 h. The solution was then cooled, filtered, and concentrated to give the desired product **3b** as a red oil. This was further purified by chromatography on silica using hexane as the eluent to give 22 mg (44%). <sup>1</sup>H NMR ( $\text{CDCl}_3$ , 500 MHz):  $\delta$  8.08 (dd,  $J = 0.75$  Hz, 8 Hz, 1H), 7.59 (dt,  $J = 0.5$  Hz, 8 Hz, 1H), 7.48 (dt,  $J = 0.5$  Hz, 8 Hz, 1H), 7.27 (d,  $J = 8.8$  Hz, 1H), 7.20 (d,  $J = 8.5$  Hz, 4H), 7.11 (d,  $J = 8.5$  Hz, 4H), 2.58 (t,  $J = 7.7$  Hz, 4H), 1.59 (m, 4H), 1.28 (m, 29H), 0.88 (t,  $J = 7$  Hz, 6H). <sup>13</sup>C NMR ( $\text{CDCl}_3$ , 125 MHz):  $\delta$  226.0, 153.4, 142.8, 142.3, 139.0, 132.7, 128.5, 128.2, 127.4, 125.0, 35.5, 31.9, 31.3, 29.6, 29.5, 29.4, 29.3, 22.7, 14.1. MALDI–FTMS ( $\text{M} + \text{H}^+$ ). Calcd for  $\text{C}_{40}\text{H}_{54}\text{S}_2$ : 599.3739. Found: 599.3742.

**General Procedure for Thiophilic Metal Precipitation.** A 10  $\mu\text{L}$  aliquot of a 200 mM stock of metal ion in water was incubated at room temperature with 200  $\mu\text{L}$  of a 10 mM stock of ligand **3a** in  $\text{CH}_3\text{CN}$ . Red precipitates from **3a** appeared upon increasing the amount of water in the final reaction mixture to over 20% (v/v). The formation of these red precipitates provided an ideal tool for verification of sample quality. Red precipitates from **3a** were readily removed by triturating the precipitate with acetonitrile.

The lack in solubility of the complexes of **4a** ( $\text{M} = \text{Hg}^{2+}$ ,  $\text{Pb}^{2+}$ , and  $\text{Cd}^{2+}$ ) not only offered metal selection but also allowed one to increase the selectivity of the method as trituration could be used to remove more soluble complexes. For instance,  $\text{Mo}^{2+}$  complexes of **3a** were readily extracted from  $\text{Hg}^{2+}$  complexes **4a** by trituration with hot 10% acetic acid. Spectroscopic analyses indicated that the rate of precipitation did not correlate with the  $K_{\text{sp}}$  and was as given by  $\text{Hg}^{2+} > \text{Pb}^{2+} > \text{Cd}^{2+} > (\text{Au}^{3+} \sim \text{Cu}^{2+}) > (\text{Pd}^{2+} \sim \text{Ni}^{2+}) > (\text{Co}^{2+} \sim \text{Mo}^{2+} \sim \text{Pt}^{2+})$ .

**Determination of the Extent of Metal Precipitation.** A 167  $\mu\text{L}$  aliquot of a 20 mM stock of  $\text{Hg}(\text{OAc})_2$  in water was incubated at room temperature with 333  $\mu\text{L}$  of a 10 mM stock of ligand **3** in  $\text{CH}_3\text{CN}$ . Precipitation occurred immediately. After 5 min the sample was centrifuged for 5 min at 14000g. The supernatant was removed and an aliquot submitted to vapor atomic absorption analysis (Galbraith Laboratories, Knoxville, TN).

**Determination of Solubility Products ( $K_{\text{sp}}$ ). (1) Weight Analysis (Figure 2A).**  $K_{\text{sp}}$  values were determined by weighing the amount of precipitate **4a**. Scaleup was required to provide sufficient material for analysis on conventional microbalances. The following procedure was used for this analysis: a 100  $\mu\text{L}$  aliquot of a 200 mM stock of metal

ion in water was incubated at room temperature with 2 mL of a 10 mM stock of ligand **3a** in acetonitrile. After 10 min the precipitate was isolated by centrifugation for 5 min at 2000g, washed with acetonitrile (5 mL) and methanol (5 mL), and dried in vacuo.

**(2) Spectrophotometric Analysis (Figure 2B).** A 10  $\mu\text{L}$  aliquot of a 200 mM stock of metal ion in water was added to 200  $\mu\text{L}$  of a 10 mM stock of ligand **3a** in acetonitrile in a spin filter (Millipore). After 10 min at room temperature, the precipitate was removed by centrifugation at 2000g. Spectroscopic analysis of the supernatant was performed on a conventional microarray reader (PerSeptive Biosystems CytoFluor or Perkin-Elmer HST 7000 plate reader).

**Heavy Metal Competitions.** A 167  $\mu\text{L}$  aliquot of a 20 mM stock of metal ion in water was incubated at room temperature with 333  $\mu\text{L}$  of a 10 mM stock of ligand **3a** in acetonitrile. After 10 min the sample was centrifuged for 5 min at 2000g or filtered through a 0.8  $\mu\text{m}$  filter plate. The supernatant was analyzed on a PerSeptive Biosystems CytoFluor or Perkin-Elmer HST 7000 plate reader using excitation at 510 nm. The metals presented were prepared using LiCl (EM Chemicals OmniPure), NaCl (Baker), KCl (EM), CsCl (Aldrich),  $\text{MgCl}_2 \cdot 6\text{H}_2\text{O}$  (EM),  $\text{CaCl}_2 \cdot 2\text{H}_2\text{O}$  (EM),  $\text{Ba}(\text{OAc})_2$  (Alfa AESAR),  $\text{VCl}_3$  (Alfa),  $\text{CrCl}_3 \cdot 6\text{H}_2\text{O}$  (EMD Chemicals),  $\text{MoCl}_3$  (Alfa),  $\text{Mn}(\text{OAc})_2$  (Alfa),  $\text{FeCl}_3 \cdot 6\text{H}_2\text{O}$  (EMD),  $\text{CoCl}_2 \cdot 6\text{H}_2\text{O}$  (Aldrich),  $\text{RhCl}_3$  (Alfa),  $\text{NiCl}_2 \cdot 6\text{H}_2\text{O}$  (Aldrich),  $\text{PdCl}_2$  (Alfa),  $\text{PtCl}_2$  (Alfa),  $\text{CuCl}_2$  (EMD),  $\text{AgCl}$  (Aldrich),  $\text{AuCl}_3$  (ICN),  $\text{ZnCl}_2$  (EMD),  $\text{CdCl}_2$  (EMD),  $\text{HgCl}_2$  (Aldrich),  $\text{Al}(\text{OAc})_3$  (Alfa),  $\text{Sn}(\text{OAc})_2$  (Alfa),  $\text{Pb}(\text{OAc})_2 \cdot 3\text{H}_2\text{O}$  (EMD),  $\text{AsCl}_3$  (Aldrich),  $\text{SbCl}_3$  (Alfa),  $\text{BiCl}_3$  (Alfa),  $\text{La}(\text{OAc})_3$  (Aldrich),  $\text{CeCl}_3$  (Aldrich),  $\text{Sm}(\text{OAc})_3$  (Aldrich),  $\text{Eu}(\text{OAc})_3$  (Aldrich), and  $\text{Yb}(\text{OAc})_3$  (Aldrich).

**Fluorescent Doping of Precipitation Reactions.** Fluorescent complexes **4a** were prepared by the addition of 200 mM metal in water to 1 mM **3a** in the presence of 5  $\mu\text{M}$  Rhod5N (Molecular Probes R-14207) or 5  $\mu\text{M}$  rhodamine B. Advantageously, the addition of Rhod5N or rhodamine B led to the formation of needles or globular crystals. Doping the reactions in this manner reduced the amount of dye required while providing sufficient fluorescence for analysis on a fluorescence microscope (Nikon Eclipse TE300). After aggregating on the glass surface, the precipitate was then washed with  $\text{H}_2\text{O}$  ( $3 \times 300 \mu\text{L}$ ). A Nikon Eclipse TE300 was used for this study. White light images were collected using Hoffman Modulation Contrast at  $100\times$  or  $1000\times$ . Fluorescent images were collected using Y-2E/C (560BP40 excitation and 595 LP 630/60 BP emission) filter.

**Displacement Map Analysis.** Positioning of the 1000 regions of each well was regulated by the assistance of an XY stage (XY stage 85–16, Linos). Precise movements ( $\pm 5 \mu\text{m}$ ) about the surface of the well were regulated by mounting the sample on the XY stage and attaching this stage to the microscope using a small (10  $\text{cm}^2$ ) microbench. A digital micrometer could be added for automation. The predicted volume was calculated by multiplying the number of microspheres by bead volume. Microspheres such as 30–100  $\mu\text{m}$  of poly(methyl methacrylate) (Sigma) or polystyrene microspheres (Sigma) were routinely for this analysis.

While analytical determinations of precipitation can be preformed in laboratory settings using microbalances or spectroscopic analysis, such machines are far too expensive for remote applications. To solve this problem, we developed a digital displacement routine to determine the volume, and hence the weight, of precipitate. This technique was based on conventional 3D volume analysis tools that use Delaunay triangulation projections to generate a 3D mesh from a 2D image.

The volume of the resulting 3D meshes was determined using conventional space-filling algorithms. As shown in Figures 3A,B, D-meshes provide an accurate representation of their 2D microscopic image.

The accuracy of this method was established by comparing a simple CCD camera (Digital Blue) to an inverted microscope (Nikon Eclipse TE300). Assays were conducted in wells (surface area of 0.9  $\text{cm}^2$ ) of a chamber slide system (Lab-Tek\*). To reduce optical errors, the bottom of each reaction well was divided into 1000 individual 300  $\mu\text{m} \times 300 \mu\text{m}$  regions and each region was filmed at 20 frames for 5 s. Each film was compiled into a single image using a scatter correction algorithm and processed using displacement map analysis. The volume of precipitate found in each region was tabulated, and the amount of precipitate found per assay was determined by summation. Calibrations using 100  $\mu\text{m}$  microspheres indicated that the Digital Blue camera provided only modest accuracy, delivering a volume of precipitate that deviated within 6% of the predicted volume, as compared to 4% for the inverted microscope. This method was then used to determine the  $K_{\text{sp}}$  of metal complexes **4a**. The error in the  $K_{\text{sp}}$  the CCD camera was only modestly greater than that obtained with the inverted microscope. Although this error was considerable, the method was far more sensitive than visual analysis, and thereby provided an effective system for analyses in nonlaboratory settings.

**Capillary Analysis of Heavy Metal Precipitation.** A 50  $\mu\text{L}$  aliquot of a stock solution of  $\text{Hg}(\text{OAc})_2$  (10 mM) and Rhod-5N (50  $\mu\text{M}$ ; Molecular Probes R-14207) in  $\text{H}_2\text{O}$  was added to 100  $\mu\text{L}$  of a 10 mM ligand **3a** stock in  $\text{CH}_3\text{CN}$ . Immediately after mixing, a sample of this solution was loaded into a 1 mm long segment of a 10  $\mu\text{m}$  i.d. capillary (Polymicro Technologies Ltd.). The loading was conducted under a microscope to ensure that crystal formation occurred after reaction within the capillary. After incubation at room temperature for 15 min, the capillary was imaged using both an inverted and conventional fluorescent microscopes.

The material requirements of this assay were reduced using micrometer-sized capillaries. Fluorescent crystals of **4a** ( $M = \text{Hg}$ ) were generated in capillaries by placing a  $1 \pm 0.05$  mm long section of 10  $\mu\text{m}$  i.d. fused silica capillary (Polymicro Technologies Inc.) containing 200  $\mu\text{M}$  **3a** and 2  $\mu\text{M}$  rhodamine B in acetonitrile into a 100  $\mu\text{L}$  aliquot of aqueous metal ion. Single or multiple crystals of **4a** were generated by placing capillaries loaded with **3a** and dye into aqueous solutions containing 0.2 nM  $\text{Hg}^{2+}$ . Using displacement map analysis, the capillary used for the experiment contained  $16.5 \pm 2.9$  fmol of **4a**. Assuming a 1:1 metal to ligand complex in **4a**, this represented the detection of  $0.17 \pm 0.3$  nM  $\text{Hg}^{2+}$  (0.3 ppb). This finding indicated an 82% yield of **4a** upon exposure to a 100  $\mu\text{L}$  aliquot of 0.2 nM  $\text{Hg}^{2+}$ . Using the same capillaries, precipitates were obtained when exposed to solutions that contained greater than 0.2 nM (0.4 ppb)  $\text{Hg}^{2+}$ , 1.5 nM (0.31 ppb)  $\text{Pb}^{2+}$ , or 2.5 nM (0.28 ppb)  $\text{Cd}^{2+}$ .

**Acknowledgment.** The authors are grateful to Dr. Olivier Pertz and Prof. Klaus Hahn for microscopy assistance and for financial support from The Skaggs Institute for Chemical Biology, an Eli Lilly Graduate Fellowship, and a Norton B. Gilula Graduate Student Fellowship.

JA045798R